

## ESR Spectra of Six-coordinate Cobalt(III) Tetraphenylporphyrin Cation Radicals Generated by Electrochemical Oxidation

Hiroaki OHYA-NISHIGUCHI,\* Masahiro KHONO,<sup>†</sup> and Kiyoko YAMAMOTO<sup>††</sup>

Department of Chemistry, Faculty of Science, Kyoto University, Sakyo-ku, Kyoto 606

<sup>†</sup> JEOL Ltd., Akishima, Tokyo 196

<sup>††</sup> The Institute of Physical and Chemical Research, Wako, Saitama 351

(Received November 19, 1980)

The ESR spectra of the paramagnetic species generated electrochemically from  $\alpha,\beta,\gamma,\delta$ -tetraphenylporphinatocobalt(II),  $[\text{Co}^{\text{II}}(\text{tpp})]$ , have been observed under the conditions of low-temperature, in chlorinated or non-chlorinated solvents, and in the presence of various supporting electrolytes. From the ESR parameters obtained, three different paramagnetic species,  $[\text{Co}^{\text{III}}(\text{tpp})]^{2+}(\text{X}^-)_2$ ,  $[\text{Co}^{\text{III}}(\text{tpp})]^{2+}(\text{Y}^-)_2$ , and  $[\text{Co}^{\text{III}}(\text{tpp})]^{2+}(\text{X}^-)(\text{Y}^-)$ , have been confirmed. The ESR spectrum of thermally and optically accessible paramagnetic species in the solution of chlorotetraphenylporphinatocobalt(III) has been reproduced by the pertinent combination of solvent and supporting electrolyte, and well interpreted by assuming the formation of  $[\text{Co}^{\text{III}}(\text{tpp})]^{2+}(\text{Cl}^-)_2$ . Arguing from a correlation between the hfcc of cobalt and nitrogen nuclei in this species, a spin-polarization mechanism is proposed to interpret the cobalt hfcc.

The application of electrochemical techniques to the study of biologically important metal-complexes has some advantages over the usual physico-chemical techniques: One is a selective formation of paramagnetic species by applying a pertinent potential comparable to the polarographic half-wave potential ( $E_{1/2}$ ) of the compound under consideration, and another is a close correlation of the electrochemical reaction with the biological redox reactions.<sup>1,2)</sup> On the other hand, the ESR measurements are very powerful for the detection of paramagnetic species.<sup>2,3)</sup> It is quite natural, therefore, to combine these techniques for a more quantitative investigation of the metal-complexes.

One of the present authors (H.O.) recently developed a simple two-electrode cell using a helix for variable temperature ESR measurements which has several advantages over the commonly used electrolysis cell for ESR in obtaining the spectra of unstable radicals.<sup>4)</sup> Using the cell, we have succeeded in obtaining ESR spectra from which the paramagnetic species oxidized electrochemically in the solution of  $[\text{Co}^{\text{II}}(\text{tpp})]$  could be identified as a  $\pi$ -cation radical of six-coordinate  $[\text{Co}^{\text{III}}(\text{tpp})]^{2+}$  having two axial ligands.

It has been reported previously<sup>5)</sup> that  $[\text{Co}^{\text{III}}(\text{tpp})]^+(\text{Cl}^-)$  is a five-coordinate Co(III) complex of tpp which has a square-pyramidal structure with the chlorine atom at the apex. Subsequent <sup>1</sup>H FT-NMR<sup>6)</sup> and ESR<sup>7)</sup> studies have shown that this complex in chlorinated solvents changes partially into paramagnetic species by thermal and light activations. The formation of this species in the solutions occurs reversibly with small enthalpy difference. Such behavior of  $[\text{Co}^{\text{III}}(\text{tpp})]^+(\text{Cl}^-)$  can be related to the enzymatic reactions of metalloporphyrins and their related compounds. In order to obtain a complete understanding about the behavior of  $[\text{Co}^{\text{III}}(\text{tpp})]^+(\text{Cl}^-)$ , it is necessary first to identify the paramagnetic species generated thermally in the solution of the complex. Secondly it is desirable to determine the molecular and electronic structures of this species.

In this paper we first describe the three kinds of spectra obtained by electrochemical oxidation of  $[\text{Co}^{\text{II}}(\text{tpp})]$  and  $[\text{Co}^{\text{III}}(\text{tpp})]^+(\text{Cl}^-)$  in chlorinated and non-chlorinated solvents, using various supporting elec-

trolytes, and explain the results by an axial-ligand effect on the  $\pi$ -cation radical of  $[\text{Co}^{\text{III}}(\text{tpp})]^{2+}$ . Secondly, the identification of the paramagnetic species formed thermally in the solution of  $[\text{Co}^{\text{III}}(\text{tpp})]^+(\text{Cl}^-)$  is given. Thirdly, the molecular and electronic structures of the species are discussed based on the ESR parameters obtained experimentally.

Model compounds such as are treated here are sometimes amenable to a more detailed ESR investigation than the biological system itself. Therefore the definitive ESR characterization of the compound can provide a framework for understanding the spin states and the electronic structures of active sites of the biological system.

### Experimental

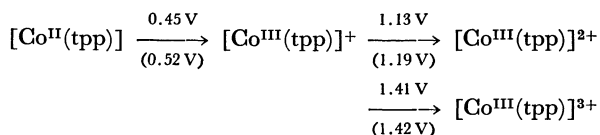
$[\text{Co}^{\text{II}}(\text{tpp})]$ ,  $[\text{Co}^{\text{III}}(\text{tpp})]^+(\text{Cl}^-)$ , and pyridine-coordinated  $[\text{Co}^{\text{III}}(\text{tpp})]^+(\text{Cl}^-)$ ,  $[\text{Co}^{\text{III}}(\text{tpp})]^+(\text{Cl}^-)(\text{py})$ , were prepared using the methods described previously.<sup>5,8)</sup> They were identified by elemental analysis and absorption spectra. Commercially available dichloromethane(DCM), 1,1,2,2-tetrachloroethane(TCE), and propionitrile(PCN) of special grade were dried with Woelm 200 neutral alumina. Tetrabutylammonium chloride(TBCL), tetrabutylammonium tetrafluoroborate(TBFB) of special grade for polarography were dried in vacuo before use. Electrochemical oxidation of  $10^{-2}$  mol solution flushed with pure nitrogen gas after degassing by the freeze-thaw-pumping cycle was carried out inside the cavity, using the cell consisting of a helix and a gold wire going through the inside of the helix. The details of the cell construction were given previously.<sup>4)</sup> It should be noted here that no reference electrode was used, in order to simplify the electrolysis apparatus. Alternatively, as an indicator of the electrochemical reactions we used the minimum voltage,  $V_a$ , applied between two electrodes, at which the ESR spectrum of the radicals generated during the electrolysis appears. The cyclic voltammogram of  $[\text{Co}^{\text{II}}(\text{tpp})]$  was measured using a Hewlett-Packard 3310A function generator in conjunction with a Princeton Applied Research 173 Potentio-Galvanostat equipped with I/V converter, Model 176. The ESR spectra were taken with a JEOL PE-3X spectrometer equipped with a temperature controller. The  $g$ -value of the Cr(III) ion in MgO used as the secondary standard for the determination of  $g$ -value was calibrated as  $1.9800 \pm 0.0001$  by that of potassium ni-

trotylbis(sulfate) ( $\text{K}_2(\text{SO}_3)_2\text{NO}$ , 2.0057).

## Results and Discussion

### Oxidation of $[\text{Co}^{\text{II}}(\text{tpp})]$ and $[\text{Co}^{\text{III}}(\text{tpp})]^+(\text{Cl}^-)$ .

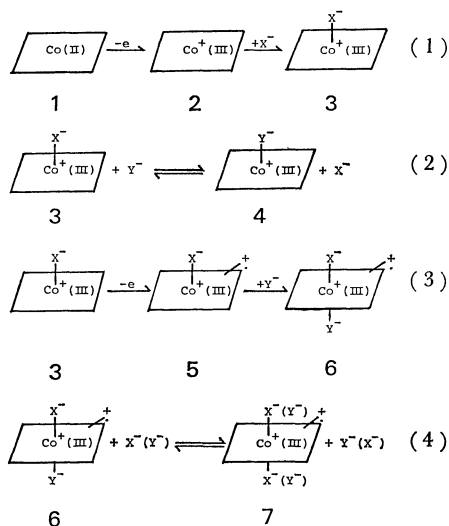
The cyclic voltammogram of  $[\text{Co}^{\text{II}}(\text{tpp})]$  in benzonitrile with TBFB showed three one-electron reversible oxidation steps corresponding to  $E_{1/2}$  vs. SCE. Here the



Scheme 1.

values in parentheses are the data reported by Wolberg and Manassen.<sup>9)</sup> The neutral species  $[\text{Co}^{\text{II}}(\text{tpp})]$  (**1**) is paramagnetic, with spin 1/2 compatible with a square-planer  $3d^7$  configuration, but can not be detected by ESR measurements in solution, because of its short spin-lattice relaxation time. The first and third oxidation products are expected to be diamagnetic species with the configurations  $(3d)^6(a_{2u})^2$  and  $(3d)^6(a_{2u})^0$ , respectively; indeed, no ESR signal was observed. Therefore, only the second oxidation product,  $[\text{Co}^{\text{III}}(\text{tpp})]^{2+}$ , takes part in the ESR spectrum.

$[\text{Co}^{\text{III}}(\text{tpp})]^+$  (**2**) requires a counter ion with which a five-coordinate complex (**3**) is expected to be formed (see Scheme 2, Eq. 1). Because **3** is diamagnetic, we can not directly observe its formation by the ESR measurements; but we can presume the formation of **3**, because the five-coordinate complex formation after one electron oxidation of **1** was well established by X-ray diffraction of  $[\text{Co}^{\text{III}}(\text{tpp})]^+(\text{Cl}^-)$  single crystal.<sup>5)</sup> Further support for Eq. 1 is available in the complexes  $[\text{M}^{\text{II}}(\text{tpp})]^+(\text{X}^-)$  ( $\text{M}=\text{Mg}$  and  $\text{Zn}$ ).<sup>10)</sup> Eq. 2 postulates an equilibrium between two five-coordinate complexes formed in the presence of two different anions in solution. If the association power of  $\text{Y}^-$  is stronger than that of  $\text{X}^-$ , the equilibrium proceeds to the right hand side of Eq. 2. When species **3** is oxidized further at the voltages between



Scheme 2.

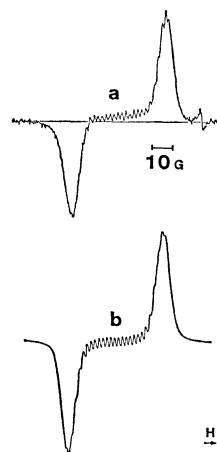


Fig. 1. The ESR spectrum of the paramagnetic species generated by electrochemical oxidation of  $[\text{Co}^{\text{II}}(\text{tpp})]$  in PCN at  $-70^\circ\text{C}$  (a). Supporting electrolyte: TBFB. Simulation (b) assumes one cobalt  $a_{\text{Co}}=6.00$  G and four nitrogens  $a_{\text{N}}=1.85$  G.

1.1 and 1.4 V SCE the first ligand oxidation proceeds (Eq. 3). In a manner similar to Eq. 1, the  $\pi$ -cation radical (**5**) produced is followed by the formation of a six-coordinate complex (**6**) with the anion  $\text{Y}^-$ . If  $\text{X}^-$  ( $\text{Y}^-$ ) exists sufficiently in excess, or the association power of  $\text{X}^-$  ( $\text{Y}^-$ ) is sufficiently stronger than that of  $\text{Y}^-$  ( $\text{X}^-$ ), the equilibrium of Eq. 4 proceeds to the right hand side. As the result of two one-electron oxidations of **1** or one-electron oxidations of **3** in various atmospheres, it is presumed that three different paramagnetic species:  $[\text{Co}^{\text{III}}(\text{tpp})]^{2+}(\text{X}^-)_2$ ,  $[\text{Co}^{\text{III}}(\text{tpp})]^{2+}(\text{X}^-)(\text{Y}^-)$ , and  $[\text{Co}^{\text{III}}(\text{tpp})]^{2+}(\text{Y}^-)_2$  are generated.

$[\text{Co}^{\text{III}}(\text{tpp})]^{2+}(\text{X}^-)_2$  ( $\text{X}=\text{BF}_4$  and  $\text{ClO}_4$ ). **1** was dissolved in chlorinated solvent, DCM or TCE, or non-chlorinated solvent, PCN, including a supporting electrolyte with a weak-ligand anion such as  $\text{ClO}_4^-$  or  $\text{BF}_4^-$ . After the temperature of the solution of PCN with  $\text{BF}_4^-$  was decreased to  $-70^\circ\text{C}$ , the voltage applied between the two electrodes was increased until the ESR signal could be observed on a recorder with the modulation amplitude of 4 G.\*\* As the voltage reached  $V_a$ , corresponding to the second oxidation, an ESR signal ( $g=2.0034$ ) with partially resolved hyperfine structure (hfs) appeared, as shown in Fig. 1a.  $V_a$  depended on the combination of solvent and supporting electrolyte.<sup>4)</sup> For example, 2.5 V for PCN with  $\text{BF}_4^-$  or  $\text{ClO}_4^-$ , 1.7 V for DCM with  $\text{BF}_4^-$ , and 1.3 V for TCE with  $\text{BF}_4^-$ . When the temperature was increased to  $-50^\circ\text{C}$ , the spectrum showed appreciable broadening and coincided with that reported in the literature.<sup>9)</sup> When DCM and TBPC(TBFB) were used as solvent and supporting electrolyte, respectively, the  $g$ -value and the hyperfine coupling constant(hfcc) of  $^{59}\text{Co}$  of the spectrum were very similar (see Table 1). As the temperature of the solution was increased above  $-50^\circ\text{C}$ , a new signal superposed to the original one appeared. The  $g$ -value and the peak-to-peak width  $\Delta H$  of this signal were

\*\* 1 G =  $10^{-4}$  T,

TABLE 1. ESR PARAMETERS OF  $[\text{Co}^{\text{III}}(\text{tpp})]^{2+}(\text{X})(\text{Y})$  AT  $-70^\circ\text{C}$ 

Axial ligands		Solvent	$g$ ( $\pm 0.0002$ )	$\Delta H^{\text{a}}$ $10^{-4}\text{ T}$	hfcc/ $10^{-4}\text{ T}$		
X	Y				Co	N	$^{35}\text{Cl}$
$\text{BF}_4^-$	$\text{BF}_4^-$	DCM	2.0024	39.6	5.3	—	—
$\text{ClO}_4^-$	$\text{ClO}_4^-$	DCM	2.0026	37.7	5.0	—	—
$\text{BF}_4^-$	$\text{BF}_4^-$	PCN	2.0034	44.6	6.0	1.85	—
$\text{ClO}_4^-$	$\text{ClO}_4^-$	PCN	2.0034	44.7	6.0	1.85	—
$\text{Cl}^-$	$\text{Cl}^-$	DCM	2.0028	80	10.3	2.8	2.2
		(DCM	2.0029	82)			
$\text{Cl}^-$	$\text{Cl}^-$	PCN	2.0035	85.5	11.0	2.6	2.2
$\text{Cl}^-$	$\text{Cl}^-$	TCE <sup>b)</sup>	2.0047	79.0	10.0	—	—
		(TCE	2.0048	77)			
$\text{BF}_4^-$	$\text{Cl}^-$	DCM	2.0052	49.0	6.6	—	—
py	$\text{Cl}^-$	DCM	2.0056	63.8	8.0		

a) Total peak-to-peak width including hfcc. b) Data at room temperature. The values in parentheses are the data of the paramagnetic species in the solution of  $[\text{Co}^{\text{III}}(\text{tpp})]^+(\text{Cl}^-)$ .

2.0052 and 49 G, respectively. This paramagnetic species was identified as a mixed-ligand complex attached by one chlorine anion, as will be discussed later.

The small variations of the hfcc of cobalt and  $g$ -values in Table 1 can be attributed to the solvent and axial-ligand effect, as was extensively investigated in the ion-pairs of aromatic hydrocarbon anion radicals with counter ions.<sup>11)</sup> The spectrum simulation of Fig. 1a was carried out using  $a_{\text{Co}}=6.0\text{ G}$  for one cobalt and  $a_{\text{N}}=1.85\text{ G}$  for four nitrogens (Fig. 1b), which led to the best fit to the experimental data. We note here that the Lorentzian line shape with the line-width of 3.5 G is used and the unresolved hfs due to eight equivalent protons of phenyl rings ( $a_{\text{H}}=0.3\text{ G}$ )<sup>11)</sup> are included; the contribution of the protons attached to the meso-phenyl rings to the line-width is also taken into account. This procedure was useful in improving the spectrum simulation. The  $g$ -value and  $a_{\text{N}}$  of this paramagnetic species are very close to those of  $[\text{M}^{\text{II}}(\text{tpp})]^+$  ( $\text{M}=\text{Mg}, \text{Zn}, \text{and Cd}$ ), as was already reviewed by Fajer and Davis.<sup>10)</sup> Such a nice coincidence of these values indicates that the paramagnetic species generated by the oxidation of **1** is a  $\pi$ -cation radical similar to  $[\text{M}^{\text{II}}(\text{tpp})]^+$ . Further, the value of  $a_{\text{N}}$  measured at temperatures below  $-60^\circ\text{C}$  guides us to the quantitative discussion of the spin distribution in the highest occupied molecular orbitals (HOMO) of the porphyrins.

$[\text{Co}^{\text{III}}(\text{tpp})]^{2+}(\text{Y}^-)_2(\text{Y}=\text{Cl})$ . The ESR spectrum of the radical obtained by the electrochemical oxidation of **1** in DCM or PCN at 1.4 V, changing the anion of electrolyte from  $\text{BF}_4^-$  ( $\text{ClO}_4^-$ ) to an intermediate-ligand,  $\text{Cl}^-$ , was somewhat different from those mentioned above. The most resolved spectrum measured at  $-70^\circ\text{C}$  is shown in Fig. 2 together with simulated ones. The spectra measured at temperatures above  $-50^\circ\text{C}$  agreed entirely with that of the paramagnetic species derived thermally from  $[\text{Co}^{\text{III}}(\text{tpp})]^+(\text{Cl}^-)$  in DCM.<sup>7)</sup> In Fig. 2a, one can recognize hfs in addition to the hfs due to  $^{59}\text{Co}$ , which could be resolved at temperatures below  $-60^\circ\text{C}$ . The hfcc were determined by comparing the observed spec-

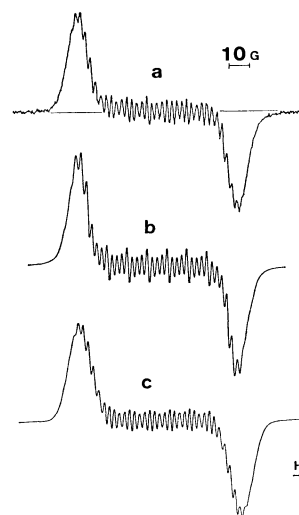


Fig. 2. The ESR spectrum of the paramagnetic species generated by electrochemical oxidation of  $[\text{Co}^{\text{II}}(\text{tpp})]$  in DCM at  $-70^\circ\text{C}$  (a). Supporting electrolyte: TBCl. Simulation (b) assumes one cobalt  $a_{\text{Co}}=10.3\text{ G}$  and four nitrogens  $a_{\text{N}}=2.80\text{ G}$ . Simulation (c) assumes one cobalt  $a_{\text{Co}}=10.3\text{ G}$ , four nitrogens  $a_{\text{N}}=2.80\text{ G}$ , and two chlorines  $a_{^{35}\text{Cl}}=2.20\text{ G}$  ( $a_{^{37}\text{Cl}}=1.80\text{ G}$ ). Contribution of the isotope to the spectrum is included.

trum with the simulated ones. Figures 2b and 2c were obtained using  $a_{\text{Co}}=10.3\text{ G}$  and  $a_{\text{N}}=2.80\text{ G}$  without and with the hfcc due to two chlorine atoms, respectively. In both cases the contribution of the unresolved proton hfcc ( $a_{\text{H}}=0.3\text{ G}$ ) is taken into account. Figure 2c was obtained by the superposition of two simulation spectra, corresponding to the existence of two chlorine isotopes ( $a_{^{35}\text{Cl}}=2.20\text{ G}$  and  $a_{^{37}\text{Cl}}=1.80\text{ G}$ ). Figure 2b is similar to the observed one, but the intensity sequences of the absorption lines and the tails of both wings of the spectrum do not coincide with the observed spectrum. The simulated spectrum, Fig. 2c, which includes the splittings due to two chlorine nuclei, coincided excellently with the observed one. The values of hfcc used for the simulations are listed in Table 1, with the measured

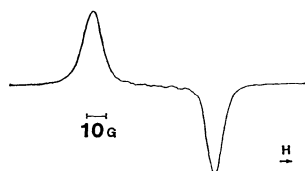


Fig. 3. The ESR spectrum of the paramagnetic species generated by electrochemical oxidation of  $[\text{Co}^{\text{III}}(\text{tpp})]^{2+}(\text{Cl}^-)(\text{py})$  in DCM at  $-90^\circ\text{C}$ . Supporting electrolyte: TBCl.

$g$ -values. The detection of the hfs due to two equivalent chlorines in addition to those due to  $^{59}\text{Co}$  and  $^{14}\text{N}$  reflects unequivocally the fact that two axial positions of **3** are occupied by chlorine anions. Thus the radical generated by the oxidation of **1** in DCM and PCN with  $\text{Cl}^-$  is identified as a  $\pi$ -cation radical of six-coordinate  $[\text{Co}^{\text{III}}(\text{tpp})]^{2+}$ , having two chlorine anions as axial ligands.

It was established in the metal complexes of meso-tetraphenylporphyrins<sup>10</sup> that meso-positions carry large spin density, whereas the nitrogen splittings ( $a_{\text{N}} = 1.2\text{--}1.9\text{ G}$ ) show about 20% of the total spin with only limited variations in  $a_{\text{N}}$ . The nitrogen hfcc in  $[\text{Co}^{\text{III}}(\text{tpp})]^{2+}(\text{Cl}^-)_2$  is a little large compared with those of  $[\text{Co}^{\text{III}}(\text{tpp})]^{2+}(\text{X}^-)_2$  ( $\text{X} = \text{BF}_4$  and  $\text{ClO}_4$ ) and of  $[\text{M}^{\text{II}}(\text{tpp})]^+(\text{M} = \text{Mg}, \text{Zn}, \text{and Cd})$ , but it is reasonable to conclude that the unpaired electron is mostly localized in  $a_{2u}$  orbital of the porphyrin ligand. The metal hfcc of 10.3 G reflects only a small unpaired electron density, of the order of 0.01.<sup>10</sup> The large  $g$ -value and  $^{59}\text{Co}$  hfcc of  $[\text{Co}^{\text{III}}(\text{tpp})]^{2+}(\text{Cl}^-)_2$ , compared with those of  $[\text{Co}^{\text{III}}(\text{tpp})]^{2+}(\text{X}^-)_2$  ( $\text{X} = \text{BF}_4$  and  $\text{ClO}_4$ ), may indicate that the chlorine ligation enhances the localization of spin density at nitrogens, which leads to the large spin polarization at the cobalt nuclei.

$[\text{Co}^{\text{III}}(\text{tpp})]^{2+}(\text{Cl}^-)(\text{Z})$  ( $\text{Z} = \text{py}$  and  $\text{BF}_4^-$ ). The possible alternative species generated by the oxidation of **1** is the one in which different ligands are present in the two axial positions. Such a configuration of the ligands could first be visualized by the oxidation of pyridine-coordinated  $[\text{Co}^{\text{III}}(\text{tpp})]^+(\text{Cl}^-)$ , in which one of the two ligand positions is strongly masked by a pyridine molecule. Figure 3 shows the spectrum of the paramagnetic species obtained by the oxidation of  $[\text{Co}^{\text{III}}(\text{tpp})]^+(\text{Cl}^-)(\text{py})$  in DCM with  $\text{Cl}^-$  ( $V_a = 2.0\text{ V}$ ). The hfs due to  $^{59}\text{Co}$  could only be resolved at temperatures below  $-50^\circ\text{C}$  ( $a_{\text{Co}} = 8.0\text{ G}$ ). The  $g$ -value, 2.0056, was appreciably larger than those described above.

The oxidation of  $[\text{Co}^{\text{III}}(\text{tpp})]^+(\text{Cl}^-)$  in DCM with  $\text{BF}_4^-$ , on the other hand, showed the spectrum due to the new radical species with  $g$ -value of 2.0052 and peak-to-peak width of 49 G, which was superimposed on that of  $[\text{Co}^{\text{III}}(\text{tpp})]^{2+}(\text{Cl}^-)_2$ . It was found from the temperature variation of the spectrum that these two species are in equilibrium. Therefore, one can conclude that the new signal corresponds to the  $[\text{Co}^{\text{III}}(\text{tpp})]^{2+}(\text{Cl}^-)(\text{BF}_4^-)$ , which shows larger  $g$ -value and smaller  $^{59}\text{Co}$  hfcc, compared with those of  $[\text{Co}^{\text{III}}(\text{tpp})]^{2+}(\text{Cl}^-)_2$ . We note here that this signal could also be observed when  $[\text{Co}^{\text{II}}(\text{tpp})]$  in DCM with  $\text{BF}_4^-$ ,

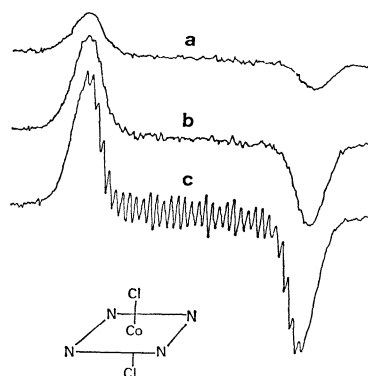
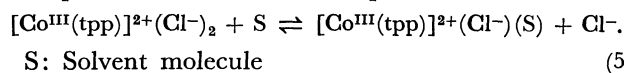


Fig. 4. Temperature dependence of the ESR spectrum of  $[\text{Co}^{\text{III}}(\text{tpp})]^{2+}(\text{Cl}^-)_2$  in DCM generated by electrochemical oxidation at  $-20$ ,  $-35$ , and  $-70^\circ\text{C}$  (a, b, and c, respectively).

the condition without chlorine anion, was oxidized at temperatures above  $-50^\circ\text{C}$ . This means that the radical subtracts the chlorine anion from the solvent used.

Consequently,  $[\text{Co}^{\text{III}}(\text{tpp})]^{2+}(\text{X}^-)_2$  ( $\text{X} = \text{BF}_4$  and  $\text{ClO}_4$ ) showed a nearly free  $g$ -value and small  $^{59}\text{Co}$  hfcc of 5.0 to 6.0 G. The  $g$ -value of  $[\text{Co}^{\text{III}}(\text{tpp})]^{2+}(\text{Cl}^-)_2$  is also very close to the free  $g$ -values, but the hfcc of  $^{59}\text{Co}$  is about twice as large as those of the former. The mixed-ligand complex can be characterized by a large  $g$ -value compared with those described above, although the value of the hfcc of  $^{59}\text{Co}$  is in the middle.

$\pi$ -Cation Radical of  $[\text{Co}^{\text{III}}(\text{tpp})]^{2+}$  Formed Thermally in the Solution of  $[\text{Co}^{\text{III}}(\text{tpp})]^+(\text{Cl}^-)$ . The solution of  $[\text{Co}^{\text{III}}(\text{tpp})]^+(\text{Cl}^-)$  in chloroform, DCM, and TCE ( $10^{-3}\text{ mol dm}^{-3}$ ) showed an ESR spectrum at room temperature even in the presence of air.<sup>7</sup> The spectrum showed reversible temperature dependence, the enthalpy difference being about  $4\text{ kJ mol}^{-1}$ . By comparing the spectrum in DCM with that of  $[\text{Co}^{\text{III}}(\text{tpp})]^{2+}(\text{Cl}^-)_2$  in DCM oxidized electrochemically at temperatures above  $-50^\circ\text{C}$ , as shown in Fig. 4, we could unequivocally identify the species as  $[\text{Co}^{\text{III}}(\text{tpp})]^{2+}(\text{Cl}^-)_2$ . On the other hand,  $[\text{Co}^{\text{III}}(\text{tpp})]^+(\text{Cl}^-)$  in TCE exhibited the temperature dependent ESR spectra, which were nicely reproduced by the electrochemical oxidation of  $[\text{Co}^{\text{III}}(\text{tpp})]^+(\text{Cl}^-)$  in TCE with  $\text{Cl}^-$ . Comparison of the ESR parameters of this spectra with those listed in Table 1 leads to an equilibrium between two species



The details of the experiments described here will be given separately.

*The Electronic Configuration of  $[\text{Co}^{\text{III}}(\text{tpp})]^{2+}$ .* As was already pointed out, the observation of the hfs due to  $^{35}\text{Cl}$  in addition to those due to  $^{59}\text{Co}$  and  $^{14}\text{N}$  led to the definite electronic structure and wave function of the radical. It was well established that the neutral species  $[\text{Co}^{\text{II}}(\text{tpp})]$  is paramagnetic with an effective electron spin 1/2 with a square-planer  $3d^7$  configuration:  $(3d_x)^4(3d_{xy})^2(3d_z)^1$ . The two-electron oxida-

tion product, on the other hand, showed definite free radical parameters which can be interpreted by a formal electronic configuration  $(3d_{\pi})^4(3d_{xy})^2(a_{2u})^1$ :  $a_{2u}$   $\pi$ -orbital has a spin distribution characterized by the appreciable localization (76%) at meso-carbon atoms, followed by 20% spin density at four nitrogen atoms. This spin distribution was experimentally confirmed by the observation of four nitrogen hfcc of 1.85 to 2.8 G in our case. The nearly free  $g$ -value of the radical tells us that 3d orbitals do not contribute to the HOMO of the radical. The almost isotropic hfcc due to  $^{59}\text{Co}$  indicates that the configuration of the central metal-ion is mainly  $(3d_{\pi})^4(3d_{xy})^2$  and the contribution to the hfcc is almost due to the Fermi contact term polarized by the spin on the neighboring  $\pi$ -orbital of the ligand.

One can consider the following mechanism to interpret  $^{59}\text{Co}$  hfcc: 1) The spin polarization of  $\sigma$ -electron in the Co-N bonds by the  $\sigma$ -electron spin density on the nitrogen nuclei produces a spin density at the cobalt nucleus: This is essentially an extension of McConnell relation<sup>12)</sup> developed originally to interpret the proton hfcc in the fragment of C-H. It should be noted that in this case the spin density at the Co nucleus is of opposite sign to that of the spin density at the  $\pi$ -orbital of the N atoms. 2) The direct overlap of the Co atomic orbital with the  $\pi$ -orbital of the ligand induces a net plus spin density at the Co nucleus. The  $\pi$ -orbital of tpp on which the unpaired electron resides has a nodal plane which coincides with the tpp molecular plane. Therefore, it is necessary to deviate from this plane for the Co atom to have the direct overlap. Then one can describe the  $a_{\text{Co}}$  as

$$a_{\text{Co}} = Q_{\text{N-Co}}^{\text{Co}} \times \rho_{\text{N}}^{\pi} + \alpha, \quad (6)$$

where  $Q_{\text{N-Co}}^{\text{Co}}$  is a proportionality constant and  $\alpha$  means a contribution from the direct overlap.

Figure 5 shows a correlation between  $a_{\text{Co}}$  and  $a_{\text{N}}$  listed in Table 1, in addition to those of other Co(III) porphyrins reported previously.<sup>9,13,14)</sup> We assume here that the sign of  $a_{\text{Co}}$  of Co(III) meso-substituted porphyrin cation radicals is negative. The data points are not so many, but one can conclude that the  $a_{\text{Co}}$  is roughly expressed by a linear function of  $a_{\text{N}}$ , which results in a linear relationship between  $a_{\text{Co}}$  and  $\rho_{\text{N}}^{\pi}$ , because  $a_{\text{N}}$  is usually expressed as  $a_{\text{N}} = Q_{\text{N}}^{\pi} \times \rho_{\text{N}}^{\pi} - \sum_i Q_{\text{NC}} \times \rho_{\text{Ci}}$  and  $\rho_{\text{Ci}} \cong 0$  for the  $a_{2u}$  orbital of tpp. It is now difficult to explain quantitatively the variation of the  $a_{\text{Co}}$  depending on the axial ligands and solvent used, but we can regard its variety as the result of the spin-polarization mechanism in the clouds of the  $a_{2u}$   $\pi$ -orbital of tpp, which changes according to the axial ligands and the solvent molecules.

## References

- 1) See, for example, P. L. Dutton and D. G. Wilson, *Biochim. Biophys. Acta*, **346**, 165 (1974); D. G. Davis, "Elec-

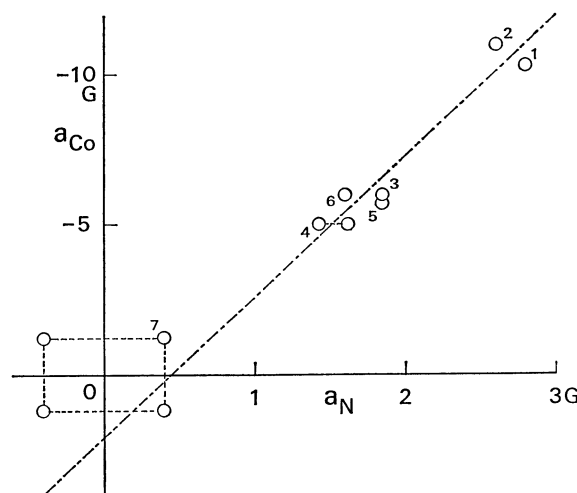


Fig. 5. A correlation between  $a_{\text{Co}}$  and  $a_{\text{N}}$  of some six-coordinate Co(III) porphyrin cation radicals; 1:  $[\text{Co}^{\text{III}}(\text{tpp})]^{2+}(\text{Cl}^-)_2$  (in DCM), 2:  $[\text{Co}^{\text{III}}(\text{tpp})]^{2+}(\text{Cl}^-)_2$  (in PCN), 3:  $[\text{Co}^{\text{III}}(\text{tpp})]^{2+}(\text{BF}_4^-)_2$  (in PCN), 4:  $[\text{Co}^{\text{III}}(\text{tpp})]^{2+}(\text{ClO}_4^-)_2$  (in DCM), 5:  $[\text{Co}^{\text{III}}(\text{tpp})]^{2+}(\text{ClO}_4^-)_2$  (in butyronitrile (BCN)), 6:  $[\text{Co}^{\text{III}}(\text{pr})_4\text{P}]^{2+}(\text{ClO}_4^-)_2$  (in BCN), and 7:  $[\text{Co}^{\text{III}}(\text{oep})]^{2+}(\text{ClO}_4^-)_2$ . For numbers 4, 5, 6, and 7,  $a_{\text{N}}$  of corresponding cation radicals of the Zn(II) complexes were used. Four points for number 7 correspond to the possibilities by the combination of the signs of  $a_{\text{Co}}$  and  $a_{\text{N}}$ .

trochemistry of Porphyrins," in "The Porphyrins," ed by D. Dolphin, Academic Press, Inc., New York and London (1978), Vol. 5, p. 127.

- 2) A. J. Hoff, *Phys. Reports*, **54**, 76 (1979).
- 3) P. F. Knowles, D. Marsh, and H. W. Rattle, "Magnetic Resonance of Biomolecules," John Wiley & Sons Ltd., London (1976), p. 168.
- 4) H. Ohya-Nishiguchi, *Bull. Chem. Soc. Jpn.*, **52**, 2064 (1979).
- 5) T. Sakurai, K. Yamamoto, H. Naito, and N. Nakamoto, *Bull. Chem. Soc. Jpn.*, **49**, 3042 (1976).
- 6) K. Yamamoto, J. Uzawa, and T. Chijimatsu, *Chem. Lett.*, **1979**, 89.
- 7) K. Yamamoto, M. Khono, and H. Ohya-Nishiguchi, *Chem. Lett.*, **1981**, 255.
- 8) K. Yamamoto and S. Tonomura, *Sci. Papers Inst. Phys. Chem. Res.*, **58**, 122 (1964).
- 9) A. Wolberg and J. Manassen, *J. Am. Chem. Soc.*, **92**, 2982 (1970).
- 10) J. Fajer and M. S. Davis, "Electron Spin Resonance of Porphyrin  $\pi$  Cations and Anions," in "The Porphyrins," ed by D. Dolphin, Academic Press, Inc., New York and London (1979), Vol. 4, p. 197.
- 11) N. Hirota, "Magnetic Resonance," ed by C. A. McDowell, Butterworths, London and Boston, (1975), Phys. Chem. Series Two, Vol. 4, p. 85.
- 12) H. M. McConnell, *J. Chem. Phys.*, **24**, 764 (1956).
- 13) D. Dolphin, A. Forman, D. C. Borg, J. Fajer, and R. H. Felton, *Proc. Natl. Acad. Sci. U.S.A.*, **68**, 614 (1971).
- 14) J. Fajer, D. C. Borg, A. Forman, A. D. Adler, and V. Varedi, *J. Am. Chem. Soc.*, **96**, 1238 (1974).